Paper Title Remodeling of pre-existing myelinated axons and oligodendrocytes is stimulated by environmental enrichment in the young adult brain

Condensed title Myelin remodeling is stimulated by environmental enrichment

Authors and author addresses

Madeline Nicholson[1], Rhiannon J Wood[1], Jessica L Fletcher[1], David G Gonsalvez [1], Anthony J Hannan[2], Simon S Murray[1.2] and Junhua Xiao[1.2] *

1. Neurotrophin and Myelin Laboratory, Department of Anatomy and Neuroscience, School of Biomedical Sciences, Faculty of Medicine, Dentistry and Health Sciences, University of Melbourne, Parkville, Victoria, 3010, Australia
2. Florey Institute of Neuroscience and Mental Health, The University of Melbourne, Parkville, Victoria, 3010, Australia

***Corresponding author** Dr. Junhua Xiao

Department of Anatomy and Neuroscience

The University of Melbourne

Victoria 3010, Australia

Tel: (+61 3) 9035 9759

Email: xiaoj@unimelb.edu.au

Conflict of interest statement

The authors declare no conflicting financial or other interests.

Author contributions

JX conceived the study; MN performed the experiments and analyzed data; RW, DG and JF assisted the experiments and data analysis; AH contributed to experimental design; JX and SM supervised the study; MN and JX wrote the manuscript.

Acknowledgements

This study was supported by Australian Research Council Discovery Project Grant (#DP180102397) to Xiao J.; the Australian Government Research Training Program

Scholarship and the University of Melbourne STRAPA Scholarship to M.N. Confocal Microscopy was performed at the Biological Optical Microscopy Platform, The University of Melbourne (www.microscopy.unimelb.edu.au).

Abstract

Neuronal activity influences oligodendrocyte production and myelination during brain development. While it is known that the myelinating process continues across the lifespan, the extent to which neuronal activity influences oligodendrocyte production and myelin acquisition during adulthood is not fully understood. Here, we find that using environmental enrichment (EE) to physiologically upregulate neuronal activity for 6-weeks during young adulthood in C57Bl/6 mice results in increased axon diameter in the corpus callosum, with a corresponding increased thickness of pre-existing myelin sheaths. Furthermore, EE uniformly promotes the differentiation of pre-existing oligodendroglia in both corpus callosum and cerebral somatosensory cortex, while differentially altering new OPC production in these regions. Together, results of this study suggest that neuronal activity induced by EE exerts a pronounced influence on adult myelination, promoting the remodeling of pre-existing myelinated axons and accelerating the differentiation of pre-existing oligodendroglia. Importantly, we show that these effects are independent of the addition of new myelin or contributions by newly-generated oligodendroglia. This impact on pre-existing oligodendroglia and pre-existing myelin sheaths is a previously undescribed form of adaptive myelination that potentially contributes to neuronal circuit maturation in the young adult central nervous system.

Introduction (4,428 characters)

Oligodendrocytes (OLs) are critical components of the central nervous system (CNS), both generating the insulating myelin sheaths that facilitate rapid transmission of action potentials along axons and providing essential metabolic and trophic support to neurons (Nave & Werner, 2014). Myelination begins developmentally and is a lifelong process, with the continued production of new OLs and generation of new myelin sheaths occurring up until middle-age (Hill, Li, & Grutzendler, 2018). Studies have revealed that the myelinating process is receptive to neuronal activity (Foster, Bujalka, & Emery, 2019) and upregulation in neuronal activity during early postnatal development increase oligodendrogenesis and myelin production, with a myelination bias towards selectively activated axons (Gibson et al., 2014; Mitew et al., 2018). Conversely, downregulations in activity via social isolation during early postnatal development decreases the number of internodes and thickness of myelin sheaths (Makinodan, Rosen, Ito, & Corfas, 2012). These experimental findings, along with computational evidence that myelination pattern variations (e.g. changes to the number, length or thickness of sheaths) can markedly alter nerve conduction velocity (Castelfranco & Hartline, 2015), identifies a role for myelin in fine-tuning neuronal connectivity. Adaptability within neuronal circuitry may influence learning and memory processes and may be important across the lifespan (Douglas Fields, 2015; Timmler & Simons, 2019).

Studies investigating the effect of neuronal activity on myelination have predominantly focused on early postnatal development and often used artificial neuronal stimulation paradigms (Gibson et al., 2014; Hill, Patel, Goncalves, Grutzendler, & Nishiyama, 2014; Makinodan et al., 2012; Mensch et al., 2015; Mitew et al., 2018). Optogenetic (Gibson et al., 2014) and pharmacogenetic (Mitew et al., 2018) methods to upregulate neuronal activity during postnatal development revealed greatly increased oligodendrocyte progenitor cell (OPC) proliferation and subsequent maturation, an affect which was recapitulated, albeit to a lesser extent, in young adult animals (Mitew et al., 2018). However, these artificial methods to upregulate neuronal stimulation to promote myelin plasticity may be problematic, as they may not actually reflect physiological levels of stimulation and have recently been shown to promote the progression of tumor growth (Venkataramani et al., 2019; Venkatesh et al., 2019). Interestingly, young adult mice (Xiao et al., 2016) and rats

(Keiner et al., 2017) that were taught complex motor paradigms exhibited an increase in new OL production, suggesting that OL adaptability extends to adulthood and is physiologically relevant. While these findings are exciting, a complete understanding of the precise changes in cellular dynamics induced by physiologically relevant stimulation and how this ultimately influences myelin in the adult CNS remains unknown. Whether increases in OL production are driven by new OPC proliferation and subsequent differentiation, or the direct differentiation of pre-existing oligodendroglia, is yet to be comprehensively assessed. Furthermore, how the maintenance and structure of existing myelin sheaths and myelinated axons is altered and how the underlying cellular changes ultimately influence new myelin generation, is unknown. This warrants a deeper exploration of how physiologically-relevant activity-induced myelination and oligodendroglial adaptations occur at post-developmental time points.

Environmental enrichment (EE) is a non-invasive and well-studied housing paradigm that provides novel and complex stimuli to the sensory, cognitive and motor systems (Nithianantharajah & Hannan, 2006). EE is known to induce neuroplasticity including promoting synaptogenesis and neurogenesis, and results in improvements in cognitive function (Nithianantharajah & Hannan, 2006). Using EE as a paradigm of physiologically relevant, upregulated neuronal activity, we investigated the generation of new myelin and the ultrastructure of existing sheaths, and comprehensively assessed the production and lineage progression of oligodendroglia, in young adult mice. We found that 6 weeks of EE did not induce significant *de novo* myelination, however we observed greatly increased axon diameters and myelin sheath thickness in the corpus callosum, indicating a remodeling of pre-existing, myelinated axons. Further, EE uniformly accelerated the lineage progression of predominantly pre-existing oligodendroglia in both the corpus callosum and cerebral somatosensory cortex regions, but differentially influenced new OPC production in these regions. Together, our data indicate that physiologically relevant neuronal stimulation in the young adult CNS induces remodeling of myelinated axons by way of axonal-caliber dependent myelinogenesis and promotes the differentiation of pre-existing oligodendroglia. Results of this study provide new insights into the dynamics of adaptive myelination in the adult CNS, opening up new questions concerning the life-long importance of myelinated axon remodeling and oligodendroglial differentiation in CNS function.

Materials and methods

Experimental animals

C57BL/6 mice were bred and housed in specific pathogen-free conditions at the Melbourne Brain Centre Animal Facility, in Techniplast IVC cages (Techniplast Group, Italy). All procedures were approved by the Florey Institute for Neuroscience and Mental Health Animal Ethics Committee following, the Australian Code of Practice for the Care and Use of Animals for Scientific Purposes.

Housing conditions and EdU administration

At 9 weeks of age, male and female animals were randomly assigned to standard or environmentally enriched housing conditions and housed single-sex with 3 mice/cage for a period of 6 weeks. Standard-housed mice remained in shoe-box sized GM500 cages (Techniplast Group, Italy) with floor area of 501cm^2. Enriched mice were moved to GR1800 double-decker cages (Techniplast Group, Italy) with floor area of 1862cm^2 and total height of 38cm. Enriched cages included a mouse-house and a selection of rubber dog toys, small plastic objects, tunnels and climbing materials. Standard-housed mice were provided only basic bedding materials and enriched mice had additional materials including shredded paper and cardboard. All cages were changed weekly with objects in enriched cages replaced, to maintain object novelty. All mice were given access to food and water ad libitum, and were on a 12-hour light/dark cycle.

Throughout the total housing period of 6 weeks, the drinking water contained thymidine analogue EdU (5-ethynyl-2'-deoxyuridine, Thermo Fisher, cat. no: E10415) to label newly-generated cells. EdU was at a concentration of 0.2mg/ml, determined previously to be non-toxic (Young et al., 2013), and refreshed every 2-3 days.

Tissue collection

Mice were anesthetized and transcardially perfused with 0.1M phosphate buffer (PBS) followed by 4% EM-grade paraformaldehyde (PFA, Electron Microscopy Sciences). Brains were dissected and post-fixed overnight in 4% PFA. The first millimeter of caudal corpus callosum was selected using a coronal mouse brain matrix and micro-dissected, then placed in Kanovsky's buffer overnight, washed in 0.1M sodium cacodylate and embedded in the

sagittal plane in epoxy resin for transmission electron microscopy (TEM) analysis. The remaining brain was rinsed in 0.1M PBS, left overnight in a 30% sucrose solution to induce cryoprotection, then embedded in OCT and snap-frozen in isopentane over dry ice, for immunohistochemistry analysis.

Immunohistochemistry and EdU labelling

20μm coronal cryosections were collected in series on SuperFrost plus slides. Sections were incubated overnight at room temperature with primary antibodies including, rabbit anti-Olig2 (Millipore, #AB9610, 1:200), mouse anti-APC/CC1 (CalBioChem, #OP-80, 1:200), and goat anti-platelet derived growth factor receptor-alpha (PDGFRα, R&D systems #AF1062, 1:200), in a PBS-based diluent buffer containing 10% normal donkey serum and 0.2% Triton-X100, then washed with 0.1M PBS and dark-incubated for 4h at room temperature with appropriate secondary antibodies including, donkey anti-rabbit 594 and donkey anti-goat 555 (Alexa Fluor, Invitrogen, 1:200) and donkey anti-mouse 405 (Abcam, ab175658, 1:200), in the same PBS-based diluent. Sections were washed with 0.1M PBS, and dark-incubated in the EdU developing cocktail prepared as per product instructions (Click-iT™ EdU Alexa Fluor™ 647 Imaging Kit, Thermo Fisher, cat. no: C10340) for 2h at room temperature, for EdU detection. Sections were washed a final time in 0.1M PBS and mounted in DAKO fluorescence mounting medium (Agilent Dako, cat. no: S3023).

Spectral unmixing confocal microscopy imaging and cell counting

Images were obtained using a 20x objective on a Zeiss LSM880 laser scanning confocal microscope with 405nm, 561nm and 633nm laser lines and Zen Black 2.3 image acquisition software. Images were taken in Lamda mode, using a ChS1 spectral GaAsP (gallium arsenide phosphide) detector to capture the entire spectrum of light, generating one image containing all fluorophores. An individual spectrum for each fluorophore was obtained by imaging control, single-stained slides and these spectra used to segregate each multi-fluorophore image into a 4-channel image, in a post-processing step under the linear un-mixing function. Uniform settings were used across experiments. Consistent regions of interest (ROI) were maintained across animals; mid-line corpus callosum and primary somatosensory cortex at approximately Bregma -1.64mm, and 3-4 images per ROI per animal were taken.

Images were manually counted by assessors blinded to housing conditions, using ImageJ/FIJI software. Oligodendroglia were defined as Olig2+, OPCs as Olig2+/ PDGFRα+ double-labelled cells, mature OLs as Olig2+/CC1+ double-labelled cells and intermediate oligodendroglia as Olig2+/CC1-/ PDGFRα-. The area of corpus callosum and somatosensory cortex was measured in each image and counts normalized.

SCoRe microscopy imaging and analysis

20μm thick coronal sections were imaged on a Zeiss LSM880 laser scanning confocal microscope with a 40x water immersion objective using 488nm, 561nm and 633nm laser lines passed through the Acousto-Optical Tunable Filters 488-640 filter/splitter and a 20/80 partially reflective mirror. Compact myelin reflected light that was then collected using three photodetectors set to collect narrow bands of light around the laser wavelengths. Uniform settings were used across experiments. Images were acquired in tile scans of 5μm z-stacks, at a minimum z-depth of 5μm from the surface. ROIs were consistent with spectral images and 3-4 images per ROI per animal were taken. Image analysis was performed in ImageJ/FIJI. Maximum intensity z-projection images were applied a minimum threshold cut-off and the resulting area of positive pixels in each ROI measured.

Transmission electron microscopy and analysis

Semi-thin (0.5-1μm) sections of caudal corpus callosum were collected on glass slides in the sagittal plane and stained with 1% toluidine blue, before subsequent ultrathin (0.1μm) sections were collected on 3x3mm copper grids. Ultrathin sections were viewed using a JEOL JEM-1400Flash TEM. Images were captured using the JEOL integrated software and a high-sensitivity sCMOS camera (JEOL Matataki Flash). Eight-ten distinct fields of view were imaged at 10,000x magnification per animal. FIJI/Image J image analysis software (National Institutes of Health) was used to count myelinated axons and the Trainable WEKA Segmentation plugin (Leslie & Heese, 2017) used to segregate myelin, allowing use of the magic wand tool to measure inner and outer axon areas, to obtain axon diameter distribution and calculate g-ratios. For each animal, at least 100 axons were measured.

Resin embedding, sectioning, post-staining and EM imaging was performed at the Peter MacCallum Centre for Advanced Histology and Microscopy.

Statistical analysis

All data was analyzed and graphed in GraphPad Prism vs8 software. Data were assumed to be normally distributed and variance assumed to be equal between groups. Sample size was determined based on what is generally used in the field. EM data was analyzed using a 2-way ANOVA with Sidak's multiple comparison test or un-paired two-tailed t-test. Spectral and SCoRe imaging data was analyzed using an un-paired two-tailed t-test. Data are presented as mean ± SEM. A significance threshold *p*-value of 0.05 was used.

Results/Discussion (15,309 characters)

Environmental enrichment increases axonal caliber and promotes myelinogenesis

To physiologically induce neuronal activity, we adopted the well-established EE housing paradigm (Nithianantharajah & Hannan, 2006). Mice were housed in EE or standard-housed (SH) control conditions for a period of 6-weeks and administered the thymidine analogue EdU in the drinking water throughout to label newly-generated cells. To verify this housing paradigm, we confirmed neurogenesis in the hippocampus, a well-defined read out of EE (Nithianantharajah & Hannan, 2006). We observed a significant increase in the density of EdU+ cells in the dentate gyrus of EE mice compared to SH control mice (862 $\pm$ 108.7 cells/mm^2 compared to 453 $\pm$ 10.1 cells/mm^2, p=0.02, Student's t-test, n=3-4 mice/group, data = mean $\pm$ SEM).

We initially investigated the influence that EE exerts on myelin plasticity by assessing the myelinated area in the corpus callosum (Fig. 1A) using SCoRe microscopy, a reflection signal of compact myelin generated by incident lasers of multiple wavelengths (Schain, Hill, & Grutzendler, 2014). Analysis of the overall myelinated area detected no significant difference between EE and SH control mice in the corpus callosum (Fig. 1A, quantitated in Fig. 1C), indicative of no significant change to *de novo* myelination. Due to recent observations of continued myelin generation in the cortex throughout the lifespan (Hill et al., 2018) and acknowledgement that grey matter myelination is emerging as a key area of myelin plasticity (Timmler & Simons, 2019), we also applied SCoRe microscopy to the overlying region of the somatosensory cortex, from which the callosal projection fibers originate (Fig. 1B). Similar to the corpus callosum, we observed no significant change to the percentage area of myelin coverage following EE housing in this region (Fig. 1B, quantitated in Fig. 1D). Additional layer-specific analysis revealed that deeper cortical layers were more heavily myelinated than superficial layers (Fig. 1E, p=0.006), however no region-dependent difference was found between housing conditions. Collectively, these data suggest there is no *de novo* myelination following EE in either corpus callosum or somatosensory cortex.

To further determine if EE exerts an influence upon myelin ensheathment, we assessed myelin ultrastructure using TEM in the corpus callosum (Fig. 2A). Concordant with the SCoRe imaging data, we found no significant change in the percentage of myelinated axons between housing conditions (Fig. 2B), confirming that EE did not increase *de novo*

myelination of previously unmyelinated axons. This finding is perhaps unsurprising as by P90 the proportion of myelinated axons in the murine corpus callosum has almost peaked (Sturrock, 1980). Interestingly, analysis of the frequency distribution of myelinated axons relative to their axonal diameter showed that EE mice had a significantly larger axonal diameters compared to SH control (Fig. 2C, p=0.008). There was an approximately 30-50% reduction in the proportion of axons with small diameters (0.2-0.5μm) and a corresponding increase in the proportion of axons with large diameters (0.8-2.3μm), resulting in an overall ~30% increase in the mean diameter of myelinated axons in EE mice compared to SH control mice (Fig. 2D, p=0.02). Previous analyses of high-frequency stimulation of hippocampal neurons has shown that axon diameters can increase by ~5% upon a time scale of 10-30 minutes (Chéreau, Saraceno, Angibaud, Cattaert, & Nägerl, 2017). This finding together with our data suggest that over a sustained period of physiologically relevant stimulation, the overall axon diameter can continue to increase up to 30%. More intriguingly, in addition to axonal caliber changes we also found a significant reduction in overall g-ratios in EE mice compared to SH controls (Fig. 2E, p<0.0001), indicative of thicker myelin sheaths. This reduction in g-ratios was observed across the full range of axon diameters (Fig. 2F, p<0.0001), indicating that EE exerts an unbiased effect upon axonal growth and myelinogenesis. These observations are consistent with previous studies identifying increased corpus callosum volume following EE housing (Markham, Herting, Luszpak, Juraska, & Greenough, 2009; Zhao et al., 2012). Our results provide clear evidence that young adult CNS myelination is highly adaptive to positive environmental experiences. We demonstrate that EE exerts a significant influence upon myelinated axon plasticity in the young adult brain by selectively promoting myelin growth of existing myelin sheaths, but not increasing *de novo* myelination of unmyelinated axons.

Increasing evidence suggests that myelin remains a dynamic structure throughout the lifespan, as observed by fluctuations in internode length (Hill et al., 2018) and turnover of myelin (Lüders et al., 2019; Yeung et al., 2014), implying there are molecular substrates susceptible to adaptive regulation. Increasing myelin thickness in response to upregulated neuronal activity may be critical in meeting enhanced metabolic demands of axons (Fünfschilling et al., 2012; Lee et al., 2012; Saab et al., 2016) and emerging evidence suggests this is necessary in sustaining function of highly active circuits (Moore et al., 2019).

A recent study has demonstrated activity-dependent localization of myelin protein mbpa mRNA within developing myelin sheaths (Yergert, Hines, & Appel, 2019), indicating a potential molecular correlate of localized sheath growth. Furthermore, bi-directional fluctuations in myelin thickness would be important in enabling adaptive responses to all manner of changing environmental conditions and indeed, myelin thinning has been observed following social isolation (Liu et al., 2012; Makinodan et al., 2012) and chronic social stress (Bonnefil et al., 2019). It is important to note that conduction velocity can be modulated by ultrastructural changes in both the axon and myelin sheath (Arancibia-Cárcamo et al., 2017; Ford et al., 2015; Waxman, 1980), which ultimately influence neuronal circuit connectivity (Ford et al., 2015; Lang, 2002) and enable adaptive-learning. Thus, in our study, the contribution of increased axonal caliber, accompanied by thicker myelin sheaths as a result of EE, to neuronal plasticity and function cannot be underestimated. The myelinated axon is a functional unit and as has been recently proposed, the term myelinated axon plasticity more accurately reflects underlying physiology (Lyons, 2017). Together with published work, our finding indicates that a positive life experience such as EE can exert a strong influence on increasing axonal caliber and the thickness of existing myelin sheaths in the adult CNS, ultimately leading to enhanced neuronal plasticity and CNS functioning, in terms of signal transmission and connectivity.

Environmental enrichment promotes the differentiation of pre-existing oligodendroglia in the corpus callosum and somatosensory cortex

To investigate whether EE influences the dynamics of OL production and integration in addition to myelin plasticity, we used spectral un-mixing confocal microscopy and comprehensively analyzed the density and proportion of all oligodendroglia, both pre-existing and newly-generated during the 6 week EE period. We assessed total oligodendroglia (Olig2+), OPCs (Olig2+/Pdgfrα+), intermediate oligodendroglia (Olig2+/Pdgfrα-/CC1-) and mature OLs (Olig2+/CC1+), distinguishing between subpopulations of pre-existing (EdU-) and newly-generated (EdU+) oligodendroglia (Fig. 3A).

To align with our myelin data, adjacent regions of corpus callosum and somatosensory cortex were analyzed. In both regions, we observed a clear significant increase in the overall density of mature OLs (callosum: Fig. 3C, p=0.02, cortex: Fig. 4B p=0.02) accompanied by a

reduction in OPCs in EE mice compared to SH controls, indicative of increased cell maturation. This effect was more pronounced in the cortex, where EE led to a significant increase in overall OL density (Fig. 4B, p=0.04) compared to SH controls. This finding is concordant with previous observations of enhanced differentiation following activity-dependent stimulation (Cullen et al., 2019; Gibson et al., 2014; Hughes, Orthmann-Murphy, Langseth, & Bergles, 2018; Keiner et al., 2017; Mitew et al., 2018; Xiao et al., 2016).

To define the altered dynamics of OL production induced by EE, we quantitated the densities of both pre-existing (EdU-) and newly-generated (EdU+) OPCs, mature OLs and intermediate oligodendroglia (callosum: Fig. 3D-E, cortex: Fig. 4C-D). We found a significantly higher density of pre-existing mature OLs in EE mice compared to SH controls (callosum: Fig. 3D, p=0.007, cortex: Fig. 4C p=0.04), suggesting that EE exerts a uniform effect upon promoting the lineage progression of pre-existing oligodendroglia, which contributes to the overall enhanced OL differentiation observed in both regions (callosum: Fig. 3C, cortex: Fig. 4B). This effect could be at least partially due to enhanced survival, as has been shown previously that EE enhances the survival of newly-generated oligodendroglia in the amygdala (Okuda et al., 2009). Furthermore, stimulating neuronal circuits via transcranial magnetic stimulation or complex motor learning results in more new pre-myelinating OLs in the motor and visual cortices (Cullen et al., 2019) or enhances the differentiation and integration of pre-existing cells (captured via EdU administration prior to paradigm onset) (Xiao et al., 2016), respectively. Thus, our finding well aligns with these published studies and suggests that providing positive experience such as EE promotes the differentiation of pre-existing oligodendroglia in the young adult brain.

We then analyzed the proportions of pre-existing (EdU-) and newly-generated (EdU+) OPCs, mature OLs and intermediate oligodendroglia in the two regions (callosum: Fig. 3F, cortex: Fig. 4E), which revealed a significant increase in the proportion of pre-existing mature OLs (callosum: Fig. 3F, overall, pre-existing: p=0.0002, p=0.0001 cortex: Fig 4E, overall, pre-existing: p=0.02, p=0.02), further confirming increased differentiation. In the corpus callosum, this was accompanied by a decrease in percentage of pre-existing intermediate oligodendroglia (Fig. 3F overall, pre-existing: p=0.008, p=0.0005), and in the cortex, a decrease in the proportion of pre-existing OPCs (Fig. 4E overall, pre-existing, p=0.02,

p=0.01). Furthermore, the proportions assessment (Fig. 3F, 4E) also revealed a reduced percentage of new OPCs in both regions (callosum: Fig. 3F, p=0.002, cortex: Fig. 4E, p=0.02) in EE mice compared to SH, suggesting that EE also promotes the direct differentiation of OPCs post-cell division. Recently, it was observed that the basal level of maturation of newly-generated OPCs in the cortex of middle-aged mice is only 22%, but incorporation of these cells can be increased 5-fold with sensory stimulation (Hughes et al., 2018), implying that the ongoing production and integration of OLs can be altered by environmental manipulations. Our data further confirm that the young adult brain contains an accessible reserve of oligodendroglia for activity-dependent responsiveness and that the lineage progression of pre-existing cells is particularly sensitive to EE stimulation. However, the main source of pre-existing oligodendroglia, intermediate or OPC, appears to be regulated differentially between the regions.

Environmental enrichment differentially regulates OPC dynamics in the corpus callosum and somatosensory cortex

Having identified that EE uniformly increases the density of mature OLs, we found a uniform decrease in the density of total OPCs in EE mice compared to SH controls, implying that the enhanced differentiation occurs at the expense of altering new OPC generation. Interestingly, we found that EE resulted in significantly fewer newly-generated OPCs in the corpus callosum (Fig. 3E p=0.001), whereas in the somatosensory cortex, this reduction is specific to pre-existing OPCs (cortex: Fig. 4C p=0.01). This finding is somewhat counterintuitive as previous studies have identified neuronal activity-dependent increases in OPC production, albeit with greatly attenuated responses observed when conducted in young adult animals (P60) (Mckenzie et al., 2014; Mitew et al., 2018) as compared to juvenile animals (P19-35) (Gibson et al., 2014; Mitew et al., 2018). These studies adopted artificial neuronal stimulation paradigms with potentially greater levels of stimulation than those induced via EE in our study, however it does suggest that age is a critical factor in the proliferative capacity of OPCs. It is also important to note that inherently, production and differentiation cannot occur simultaneously, as differentiation removes an available proliferative cell. Thus, our finding that EE results in an overall increase in mature OLs accompanied by an overall reduction in OPCs indicates that physiological stimulation of neuronal activity favorably promotes oligodendroglial differentiation, which alters the

dynamics of OPC production in the young adult brain. We have previously shown that there is a drastic decline in OPC density occurring across different CNS regions from P9-30 (Nicholson et al., 2018). Furthermore, as OPC density decreases, although they remain evenly tiled (Hughes, Kang, Fukaya, & Bergles, 2013), the probability that a cell will be in close proximity to a specifically activated axon and thus able to sense and respond to changing activity levels, is also reduced. Results from this study and others suggest that adult animals retain an ability to respond to neuronal activity and attenuated responses may be due to logistical constraints on cell numbers, rather than inhibitive cellular environments. Our finding suggests that EE accelerates the normal process of OL production and integration in the young adult brain via enhancing differentiation, ultimately resulting in a reduction in OPCs.

To further determine the differential reduction in new OPC generation we examined the proportional contributions of new vs pre-existing oligodendroglia to the pool of total oligodendroglia, OCPs, mature OLs and intermediate oligodendroglia in both regions. In the corpus callosum, the overall proportion of pre-existing oligodendroglia was significantly increased in EE mice compared to SH controls (Fig. 3G, $p=0.03$), which is reflected by increased proportions of both pre-existing OPCs (Fig. 3G, $p=0.009$) and pre-existing mature OLs (Fig. 3G, $p=0.03$). Interestingly, EE exerted no significant influence upon the relative proportions of pre-existing and new oligodendroglia in somatosensory cortex (Fig. 4F). This data demonstrates clear regional heterogeneity in response to the EE paradigm. In the corpus callosum EE reduces the contribution of newly-generated oligodendroglia by markedly increasing the direct incorporation of pre-existing oligodendroglia, whereas within the somatosensory cortex the incorporation of pre-existing oligodendroglia induced by EE does not affect the generation of new OPCs to the same extent. Cortical and callosal OPCs behave differently from early postnatal development (Nicholson et al., 2018). Furthermore, subsets of OPCs have been identified based on differential expression of ion channels and neurotransmitter receptors, and relative proportions of each subtype differ regionally (Spitzer et al., 2019), indicating a heterogenous distribution of OPCs that could partially explain the distinct response to EE.

Results of our study suggest that in the young adult brain, positive experience predominantly influences the plasticity of pre-existing oligodendroglia and existing myelin sheaths, without substantial *de novo* myelin sheath generation. Future studies concerned with myelin plasticity should attempt to distinguish between changes appearing due to generation of new OLs and new myelin sheaths, and changes appearing due to influences on pre-existing cells, axons and sheaths. This difference is subtle, yet critical in understanding the implications and relevance of adaptive myelination in animals across the lifespan from developmental, to aging stages, as well as in translating these findings for therapeutic benefit in the context of demyelinating diseases. Techniques to capture such specific changes could include methods that measure myelin generation and turnover, which were recently nicely reviewed (Buscham, Eichel, Siems, & Werner, 2019). Additionally, genetic approaches that enable inducible and OL-specific expression of a myelin-associated membrane-bound fluorescent protein (Hill & Grutzendler, 2019) in conjunction with time-lapse *in vivo* imaging, would provide a more detailed spatial and temporal analysis of the adaptive myelinating process.

In summary, we are the first to demonstrate that providing physiologically relevant neuronal stimulation via EE exerts a strong influence upon adult myelin remodeling, increasing the diameter and promoting myelin wrapping of pre-existing myelinated axons. This study provides a systematic assessment of oligodendroglial lineage dynamics in a healthy, young adult brain and importantly identifies that EE uniformly increases the differentiation of pre-existing oligodendroglia in both corpus callosum and somatosensory cortex, with a region-specific influence on new OPC generation. This contrasts with previous studies that have adopted non-physiological strategies to manipulate neuronal activity and found notable increases in new OPC production and *de novo* myelination of previously unmyelinated axons. Results of this study extend our understanding of myelinated axon plasticity and provide new insights into how altering neuronal activity at a physiological level can modulate existing axons, myelin sheaths and pre-existing oligodendroglial maturation. Findings of this study will provide a platform for future investigation into the functional importance of oligodendroglial differentiation and myelinated axon remodeling for behavior and cognition throughout the lifespan.

References

Arancibia-Cárcamo, I. L., Ford, M. C., Cossell, L., Ishida, K., Tohyama, K., & Attwell, D. (2017). Node of ranvier length as a potential regulator of myelinated axon conduction speed. *ELife*, *6*, 1–15. https://doi.org/10.7554/eLife.23329

Bonnefil, V., Dietz, K., Amatruda, M., Wentling, M., Aubry, A. V, Dupree, J. L., … Liu, J. (2019). Region-specific myelin differences define behavioral consequences of chronic social defeat stress in mice. *ELife*, *8*, 1–13. https://doi.org/10.7554/eLife.40855

Buscham, T., Eichel, M., Siems, S., & Werner, H. (2019). Turning to myelin turnover. *Neural Regeneration Research*, *14*(12), 2063. https://doi.org/10.4103/1673-5374.262569

Castelfranco, A. M., & Hartline, D. K. (2015). The evolution of vertebrate and invertebrate myelin: a theoretical computational study. *Journal of Computational Neuroscience*, *38*(3), 521–538. https://doi.org/10.1007/s10827-015-0552-x

Chéreau, R., Saraceno, G. E., Angibaud, J., Cattaert, D., & Nägerl, U. V. (2017). Superresolution imaging reveals activity-dependent plasticity of axon morphology linked to changes in action potential conduction velocity. *Proceedings of the National Academy of Sciences of the United States of America*, *114*(6), 1401–1406. https://doi.org/10.1073/pnas.1607541114

Cullen, C. L., Senesi, M., Tang, A. D., Clutterbuck, M. T., Auderset, L., O'Rourke, M. E., … Young, K. M. (2019). Low-intensity transcranial magnetic stimulation promotes the survival and maturation of newborn oligodendrocytes in the adult mouse brain. *Glia*, (March), glia.23620. https://doi.org/10.1002/glia.23620

Douglas Fields, R. (2015). A new mechanism of nervous system plasticity: activity-dependent myelination. *Nature Reviews. Neuroscience*, *16*(12), 756–767. https://doi.org/10.1038/nrn4023

Ford, M. C., Alexandrova, O., Cossell, L., Stange-Marten, A., Sinclair, J., Kopp-Scheinpflug, C., … Grothe, B. (2015). Tuning of Ranvier node and internode properties in myelinated axons to adjust action potential timing. *Nature Communications*, *6*, 8073. https://doi.org/10.1038/ncomms9073

Foster, A. Y., Bujalka, H., & Emery, B. (2019). Axoglial interactions in myelin plasticity: Evaluating the relationship between neuronal activity and oligodendrocyte dynamics. *Glia*, (February), glia.23629. https://doi.org/10.1002/glia.23629

Fünfschilling, U., Supplie, L. M., Mahad, D., Boretius, S., Saab, A. S., Edgar, J., … Nave, K. A.

(2012). Glycolytic oligodendrocytes maintain myelin and long-term axonal integrity. *Nature*, *485*(7399), 517–521. https://doi.org/10.1038/nature11007

Gibson, E. M., Purger, D., Mount, C. W., Goldstein, A. K., Lin, G. L., Wood, L. S., … Monje, M. (2014). Neuronal Activity Promotes Oligodendrogenesis and Adaptive Myelination in the Mammalian Brain. *Science*, *344*(6183), 1252304–1252304. https://doi.org/10.1126/science.1252304

Hill, R. A., & Grutzendler, J. (2019). Uncovering the biology of myelin with optical imaging of the live brain. *Glia*, (February), glia.23635. https://doi.org/10.1002/glia.23635

Hill, R. A., Li, A. M., & Grutzendler, J. (2018). Lifelong cortical myelin plasticity and age-related degeneration in the live mammalian brain. *Nature Neuroscience 2018*, *26*, 1. https://doi.org/10.1038/s41593-018-0120-6

Hill, R. A., Patel, K. D., Goncalves, C. M., Grutzendler, J., & Nishiyama, A. (2014). Modulation of oligodendrocyte generation during a critical temporal window after NG2 cell division. *Nature Neuroscience*, *17*(11), 1518–1527. https://doi.org/10.1038/nn.3815

Hughes, E. G., Kang, S. H., Fukaya, M., & Bergles, D. E. (2013). Oligodendrocyte progenitors balance growth with self-repulsion to achieve homeostasis in the adult brain. *Nature Neuroscience*, *16*(6), 668–676. https://doi.org/10.1038/nn.3390

Hughes, E. G., Orthmann-Murphy, J. L., Langseth, A. J., & Bergles, D. E. (2018). Myelin remodeling through experience-dependent oligodendrogenesis in the adult somatosensory cortex. *Nature Neuroscience 2018*, 1. https://doi.org/10.1038/s41593-018-0121-5

Keiner, S., Niv, F., Neumann, S., Steinbach, T., Schmeer, C., Hornung, K., … Redecker, C. (2017). Effect of skilled reaching training and enriched environment on generation of oligodendrocytes in the adult sensorimotor cortex and corpus callosum. *BMC Neuroscience*, *18*(1), 31. https://doi.org/10.1186/s12868-017-0347-2

Lang, E. J. (2002). Role of Myelination in the Development of a Uniform Olivocerebellar Conduction Time. *Journal of Neurophysiology*, *89*(4), 2259–2270. https://doi.org/10.1152/jn.00922.2002

Lee, Y., Morrison, B. M., Li, Y., Lengacher, S., Farah, M. H., Hoffman, P. N., … Rothstein, J. D. (2012). Oligodendroglia metabolically support axons and contribute to neurodegeneration. *Nature*, *487*(7408), 443–448. https://doi.org/10.1038/nature11314

Leslie, M. E., & Heese, A. (2017). Quantitative Analysis of Ligand-Induced Endocytosis of FLAGELLIN-SENSING 2 Using Automated Image Segmentation. In *Trends in Immunology* (Vol. 35, pp. 39–54). https://doi.org/10.1007/978-1-4939-6859-6_4

Liu, J., Dietz, K., Deloyht, J. M., Pedre, X., Kelkar, D., Kaur, J., … Casaccia, P. (2012). Impaired adult myelination in the prefrontal cortex of socially isolated mice. *Nature Neuroscience*, *15*(12), 1621–1623. https://doi.org/10.1038/nn.3263

Lüders, K. A., Nessler, S., Kusch, K., Patzig, J., Jung, R. B., Möbius, W., … Werner, H. B. (2019). Maintenance of high proteolipid protein level in adult central nervous system myelin is required to preserve the integrity of myelin and axons. *Glia*, *67*(4), 634–649. https://doi.org/10.1002/glia.23549

Lyons, D. A. (2017). On Myelinated Axon Plasticity and Neuronal Circuit Formation and Function, *37*(Xx), 10023–10034. https://doi.org/10.1523/JNEUROSCI.3185-16.2017

Makinodan, M., Rosen, K. M., Ito, S., & Corfas, G. (2012). A Critical Period for Social Experience-Dependent Oligodendrocyte Maturation and Myelination. *Science*, *337*(6100), 1357–1360. https://doi.org/10.1126/science.1220845

Markham, J. A., Herting, M. M., Luszpak, A. E., Juraska, J. M., & Greenough, W. T. (2009). Myelination of the corpus callosum in male and female rats following complex environment housing during adulthood. *Brain Research*, *1288*, 9–17. https://doi.org/10.1016/j.brainres.2009.06.087

Mckenzie, I. A., Ohayon, D., Li, H., Faria, J. P. De, Emery, B., Tohyama, K., & Richardson, W. D. (2014). Motor skill learning requires active central myelination. *Science*, *346*(6207), 318–322. https://doi.org/10.1126/science.1254960

Mensch, S., Baraban, M., Almeida, R., Czopka, T., Ausborn, J., El Manira, A., & Lyons, D. A. (2015). Synaptic vesicle release regulates myelin sheath number of individual oligodendrocytes in vivo. *Nature Neuroscience*, *18*(5), 628–630. https://doi.org/10.1038/nn.3991

Mitew, S., Gobius, I., Fenlon, L. R., Mcdougall, S., Hawkes, D., Xing, Y. L., … Emery, B. 6. (2018). Pharmacogenetic stimulation of neuronal activity increases myelination 1 in an axon-specific manner 2 3. *Nature Communications*, 1–16. https://doi.org/10.1038/s41467-017-02719-2

Moore, S., Meschkat, M., Ruhwedel, T., Tzvetanova, I. D., Trevisiol, A., Kusch, K., … Biosciences, M. (2019). A role of oligodendrocytes in information processing

independent of conduction velocity.

Nave, K.-A., & Werner, H. B. (2014). Myelination of the Nervous System: Mechanisms and Functions. *Annual Review of Cell and Developmental Biology*, *30*, 503–533. https://doi.org/10.1146/annurev-cellbio-100913-013101

Nicholson, M., Wood, R. J., Fletcher, J. L., van den Buuse, M., Murray, S. S., & Xiao, J. (2018). BDNF haploinsufficiency exerts a transient and regionally different influence upon oligodendroglial lineage cells during postnatal development. *Molecular and Cellular Neuroscience*, *90*(November 2017), 12–21. https://doi.org/10.1016/j.mcn.2018.05.005

Nithianantharajah, J., & Hannan, A. J. (2006). Enriched environments, experience-dependent plasticity and disorders of the nervous system. *Nature Reviews. Neuroscience*, *7*(9), 697–709. https://doi.org/10.1038/nrn1970

Okuda, H., Tatsumi, K., Makinodan, M., Yamauchi, T., Kishimoto, T., & Wanaka, A. (2009). Environmental enrichment stimulates progenitor cell proliferation in the amygdala. *Journal of Neuroscience Research*, *87*(16), 3546–3553. https://doi.org/10.1002/jnr.22160

Saab, A. S., Tzvetavona, I. D., Trevisiol, A., Baltan, S., Dibaj, P., Kusch, K., … Nave, K. A. (2016). Oligodendroglial NMDA Receptors Regulate Glucose Import and Axonal Energy Metabolism. *Neuron*, *91*(1), 119–132. https://doi.org/10.1016/j.neuron.2016.05.016

Schain, A. J., Hill, R. A., & Grutzendler, J. (2014). Disease With Spectral Confocal Reflectance Microscopy. *Nature Medicine*, *20*(4), 443–449. https://doi.org/10.1038/nm.3495.Label-free

Spitzer, S. O., Sitnikov, S., Kamen, Y., Evans, K. A., Kronenberg-Versteeg, D., Dietmann, S., … Káradóttir, R. T. (2019). Oligodendrocyte Progenitor Cells Become Regionally Diverse and Heterogeneous with Age. *Neuron*, *0*(0), 1–13. https://doi.org/10.1016/J.NEURON.2018.12.020

Sturrock, R. R. (1980). Myelination of the Mouse Corpus Callosum. *Neuropathology and Applied Neurobiology*, *6*(6), 415–420. https://doi.org/10.1111/j.1365-2990.1980.tb00219.x

Timmler, S., & Simons, M. (2019). Grey matter myelination. *Glia*, (January), 1–8. https://doi.org/10.1002/glia.23614

Venkataramani, V., Tanev, D. I., Strahle, C., Studier-Fischer, A., Fankhauser, L., Kessler, T., … Kuner, T. (2019). Glutamatergic synaptic input to glioma cells drives brain tumour

progression. *Nature*, *573*(7775), 532–538. https://doi.org/10.1038/s41586-019-1564-x

Venkatesh, H. S., Morishita, W., Geraghty, A. C., Silverbush, D., Gillespie, S. M., Arzt, M., … Monje, M. (2019). Electrical and synaptic integration of glioma into neural circuits. *Nature*, *573*(7775), 539–545. https://doi.org/10.1038/s41586-019-1563-y

Waxman, S. G. (1980). Determinants of conduction velocity in myelinated nerve fibers. *Muscle & Nerve*, *3*(2), 141–150. https://doi.org/10.1002/mus.880030207

Xiao, L., Ohayon, D., McKenzie, I. A., Sinclair-Wilson, A., Wright, J. L., Fudge, A. D., … Richardson, W. D. (2016). Rapid production of new oligodendrocytes is required in the earliest stages of motor-skill learning. *Nature Neuroscience*, *19*(9), 1210–1217. https://doi.org/10.1038/nn.4351

Yergert, K. M., Hines, J. H., & Appel, B. (2019). Neuronal Activity Enhances mRNA Localization to Myelin Sheaths During Development, 1–30.

Yeung, M. S. Y., Zdunek, S., Bergmann, O., Bernard, S., Salehpour, M., Alkass, K., … Fris??n, J. (2014). Dynamics of oligodendrocyte generation and myelination in the human brain. *Cell*, *159*(4), 766–774. https://doi.org/10.1016/j.cell.2014.10.011

Young, K. M., Psachoulia, K., Tripathi, R. B., Dunn, S. J., Cossell, L., Attwell, D., … Richardson, W. D. (2013). Oligodendrocyte dynamics in the healthy adult CNS: Evidence for myelin remodeling. *Neuron*, *77*(5), 873–885. https://doi.org/10.1016/j.neuron.2013.01.006

Zhao, Y.-Y., Shi, X.-Y., Qiu, X., Lu, W., Yang, S., Li, C., … Tang, Y. (2012). Enriched Environment Increases the Myelinated Nerve Fibers of Aged Rat Corpus Callosum. *The Anatomical Record: Advances in Integrative Anatomy and Evolutionary Biology*, *295*(6), 999–1005. https://doi.org/10.1002/ar.22446

Figures and figure legends

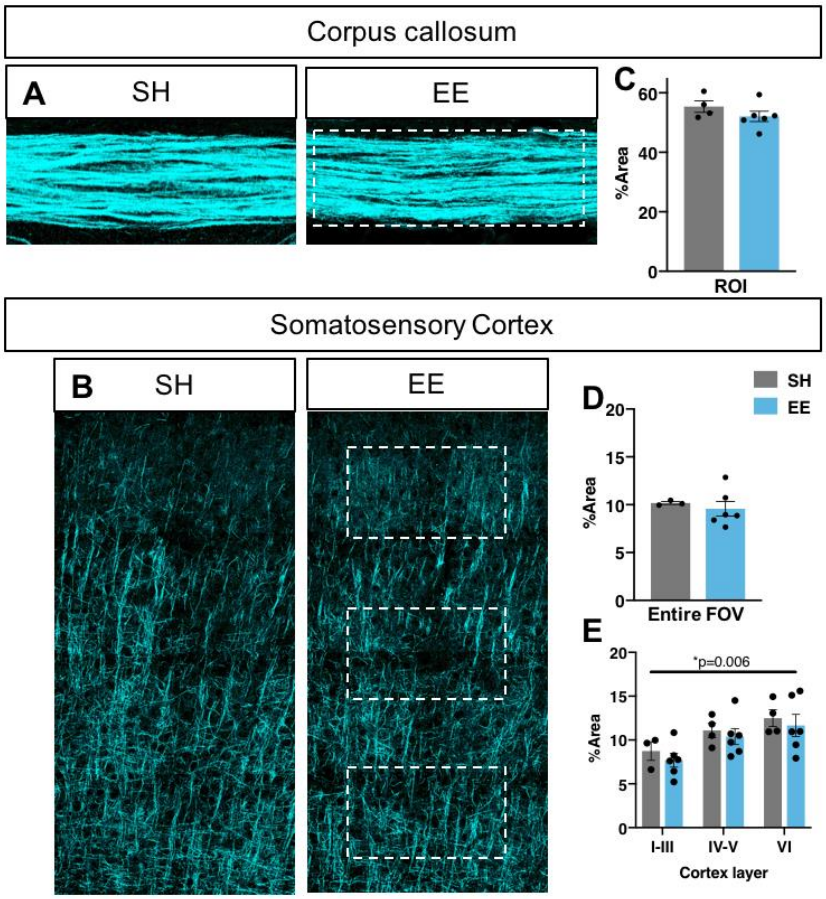

Figure 1. Environmental enrichment exerts no influence on myelinated area

(A-B) Representative SCoRe images of corpus callosum **(A)** and somatosensory cortex **(B)** of control SH mice and EE housed mice. **(C-E)** Quantification of myelinated area as per percentage area of SCoRe signal measured in a corpus callosum ROI (p=0.25, unpaired two-tailed t-test) **(C)**, across the entire somatosensory cortex (p=0.62, unpaired two-tailed t-test) **(D)** and in 3 layer-specific cortical ROIs (dotted outlines, 2-way ANOVA with Sidak's multiple comparisons) **(E)**. C-E: n=3-6 mice/group, data = mean ± SEM.

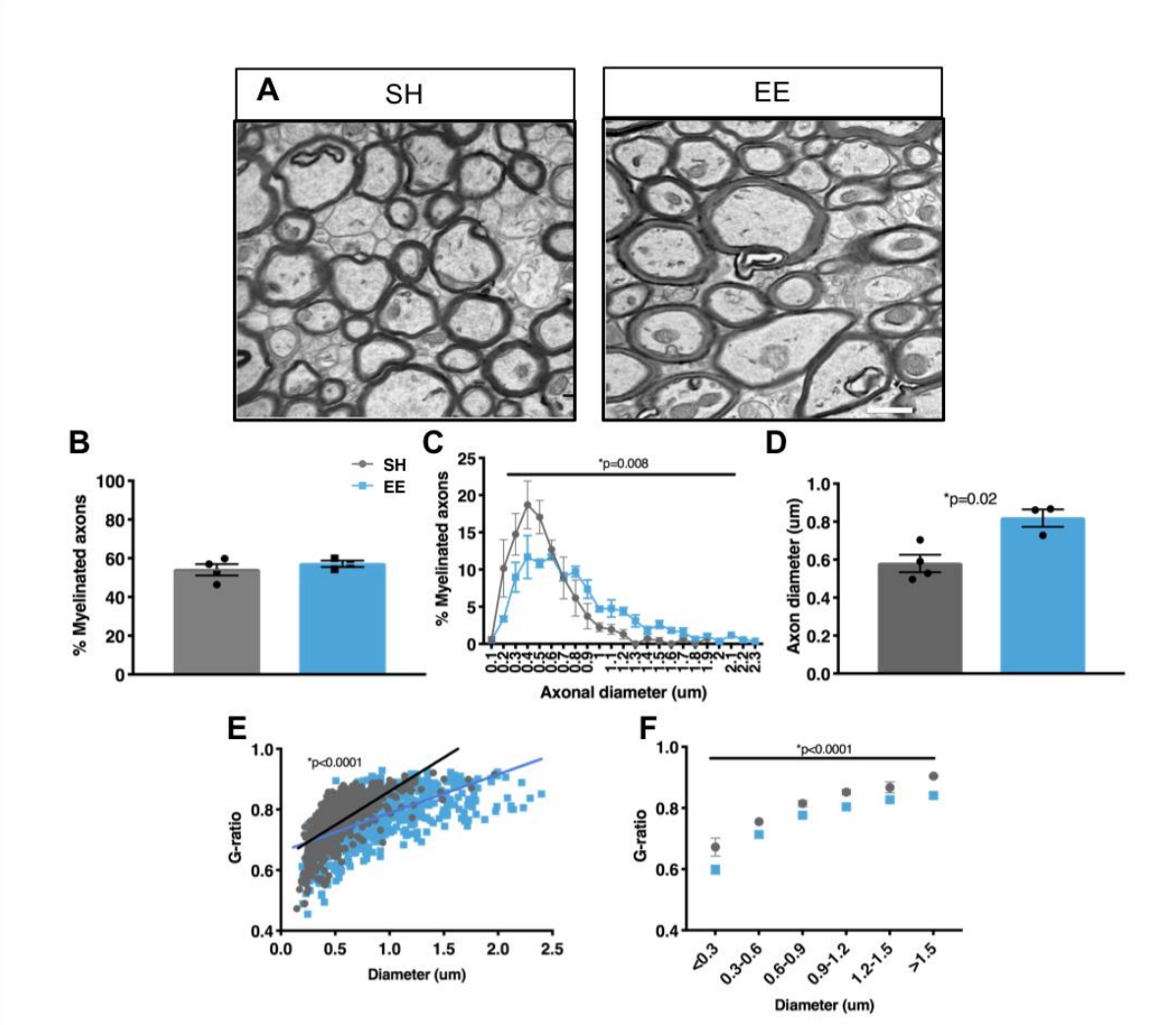

Figure 2. Environmental enrichment increases axonal caliber and promotes myelinogenesis in the corpus callosum

(A) Representative EM micrographs of caudal corpus callosum of control SH or EE housed mice. Scale bar = 1μm. **(B)** Quantification of the percentage of myelinated axons in the corpus callosum (p=0.45, unpaired two-tailed t-test). **(C)** Frequency distribution of myelinated axons relative to diameter (2-way ANOVA; interaction p=0.008). **(D)** Quantification of average axon diameter in the corpus callosum (p=0.02, unpaired two-tailed t-test). **(E)** Scatter plot of g-ratio distribution of individual axons relative to axon diameter (linear regression analysis, p<0.0001). **(F)** Plot of average g-ratio binned by axon diameter (2-way ANOVA with Sidak's multiple comparison test; factors: housing p<0.0001, diameter p<0.0001, interaction p=0.8). For C-F: >100 axons/mouse/group, n=3-4 mice/group, data = mean±SEM.

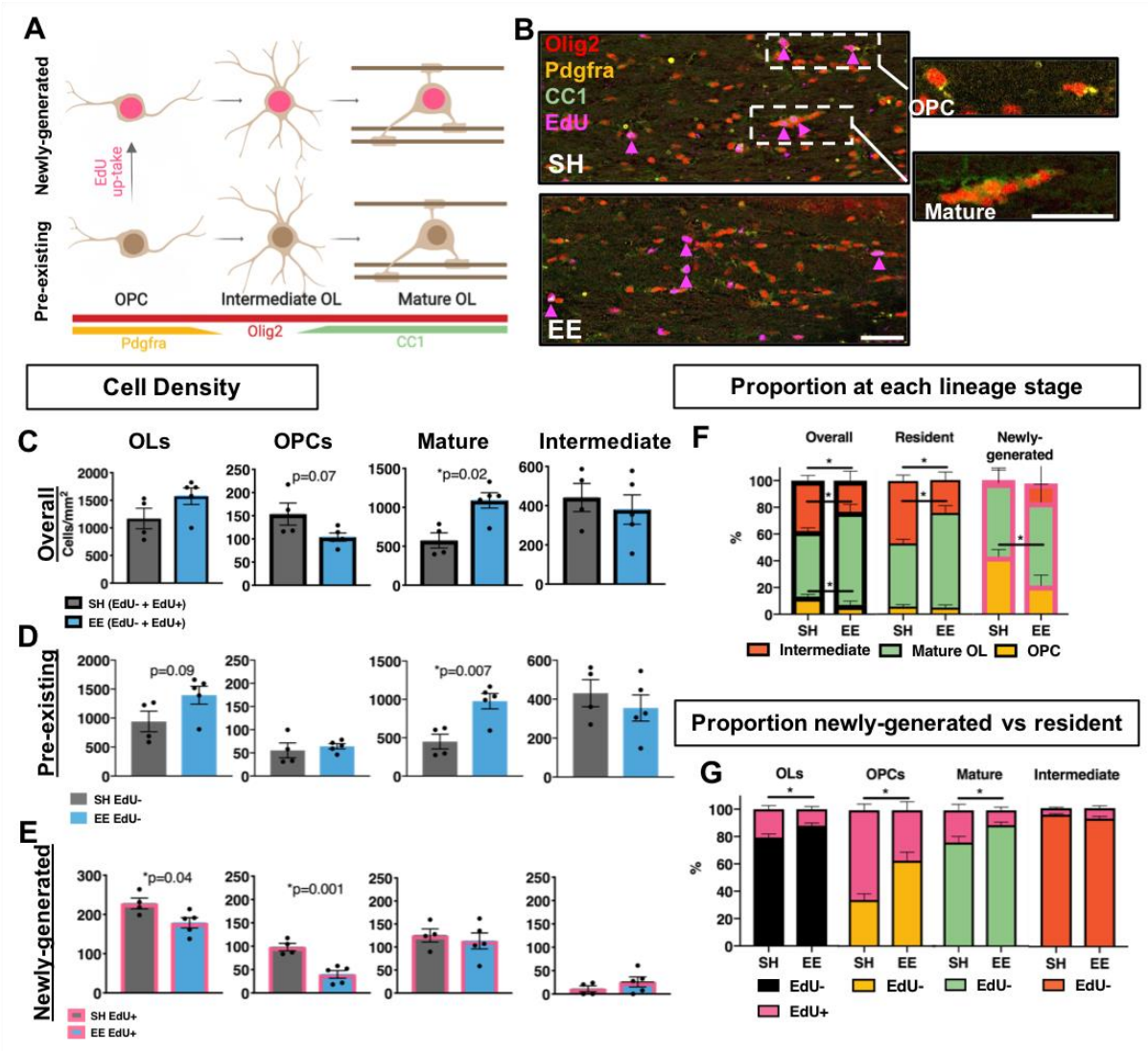

Figure 3. Environmental enrichment enhances the differentiation of pre-existing oligodendrocytes in the corpus callosum.

(A) Schematic of the markers used to label distinct stages of the oligodendroglial lineage. This image was created using BioRender.com. **(B)** Representative confocal micrographs of Olig2/EdU/PDGFRAα/CC1 quadruple-immunostaining in the corpus callosum for SH or EE housed mice. Insert from SH animal depicts new-OLs (EdU+, pink arrows), OPCs (Olig2+/PDGFRAα+) and mature OLs (Olig2+/CC1+). Scale bar = 25μm. **(C-E)** Quantification of the density of total oligodendroglia (Olig2+), as well as oligodendroglia sub-divided by lineage stage; OPCs (Olig2+/ PDGFRAα+), mature OLs (Olig2+/CC1+) and intermediate oligodendroglia (Olig2+/ PDGFRAα-/CC1-) in the corpus callosum. **(C)** Overall oligodendroglial densities [Pre-existing (EdU-) + Newly-generated (EdU+)] (OLs p=0.13, OPCs p=0.07, Mature p=0.02, Intermediate p=0.58). **(D)** Pre-existing (EdU-) oligodendroglial

densities (OLs p=0.09, OPCs p=0.58, Mature p=0.007, Intermediate p=0.46). **(E)** Newly-generated (EdU+) oligodendroglial densities (OLs p=0.04, OPCs p=0.001, Mature p=0.62, Intermediate p=0.21). **(F)** Quantification of the proportions of oligodendroglia at each stage of lineage development, for the overall population of oligodendroglia (OPCs p=0.006, Mature p=0.0002, Intermediates p=0.008), the population of pre-existing (EdU-) oligodendroglia (OPCs p=0.57, Mature p=0.0001, Intermediates p=0.0005) and the population of newly-generated (EdU+) oligodendroglia (OPCs p=0.002, Mature p=0.39, Intermediate p=0.18). **(G)** Quantification of the proportions of newly-generated (EdU+) vs pre-existing (EdU-) oligodendroglia overall (p=0.03), and at each lineage stage in the corpus callosum (OPCs p=0.009, Mature p=0.03, Intermediate p=0.30). C-G: n=4-5 mice/group, unpaired two-tailed t-test, data = mean ± SEM.

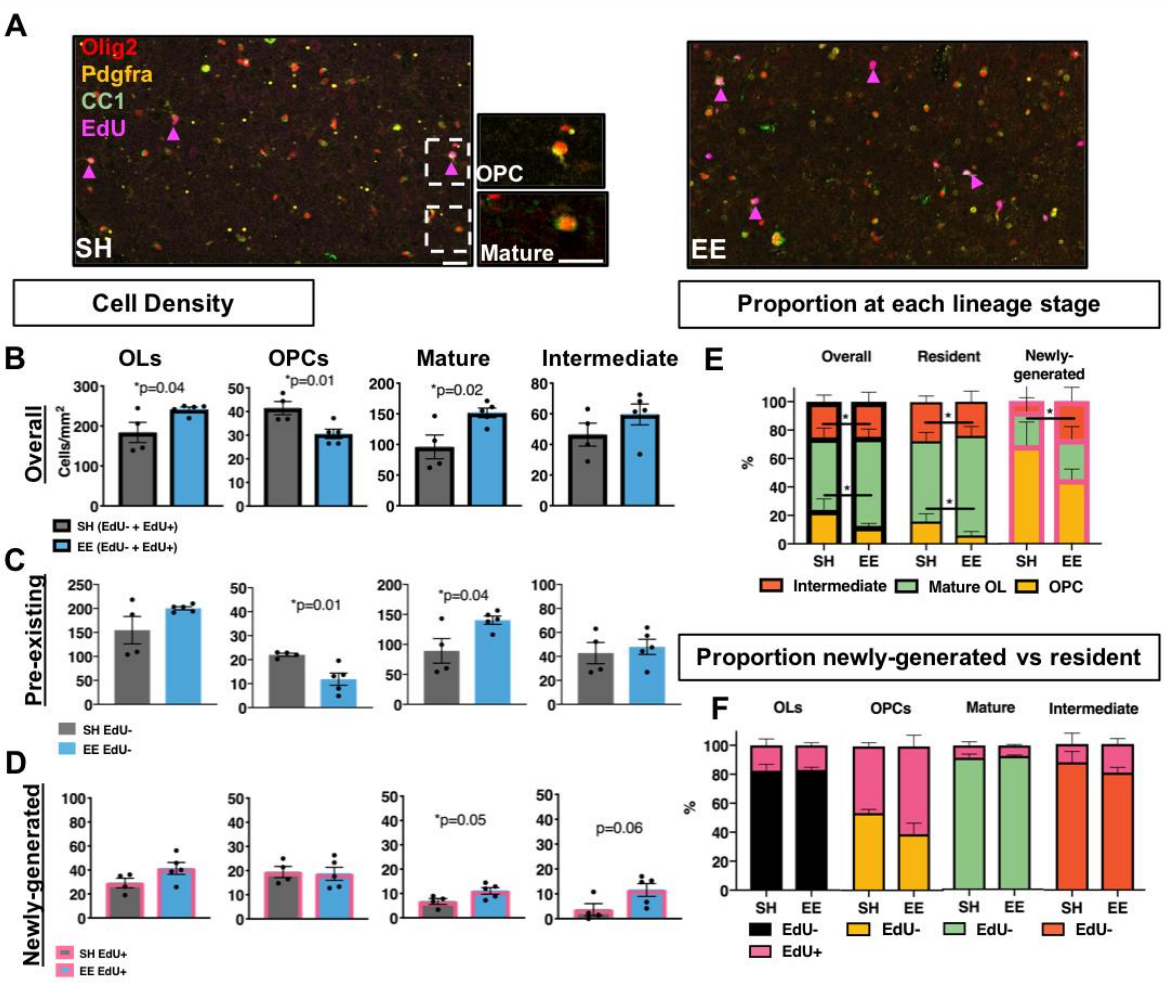

Figure 4. Environmental enrichment enhances the differentiation of pre-existing and new oligodendroglia in the somatosensory cortex.

(A) Representative confocal micrographs of Olig2/EdU/PDGFRAα/CC1 quadruple-immunostaining in the somatosensory cortex for SH or EE house mice. Insert from SH animal depicts new- oligodendroglia (EdU+, pink arrows), OPCs (Olig2+/PDGFRAα+) and mature OLs (Olig2+/CC1+). Scale bar = 25μm. **(B-D)** Quantification of the density of total oligodendroglia, as well as oligodendroglia sub-divided by lineage stage; OPCs, mature OLs and intermediate oligodendroglia in the somatosensory cortex. **(B)** Overall oligodendroglial densities (OLs p=0.04, OPCs p=0.01, Mature p=0.02, Intermediate p=0.24). **(C)** Pre-existing oligodendroglial densities (OLs p=0.11, OPCs p=0.01, Mature p=0.04, Intermediate p=0.64). **(D)** Newly-generated oligodendroglial densities (OLs p=0.11, OPCs p=0.85, Mature p=0.05, Intermediate p=0.06). **(E)** Quantification of the proportions of oligodendroglia at each stage of lineage development, for the overall population of oligodendroglia (OPCs: p=0.02, Mature: p=0.02, Intermediate p=0.9), the population of pre-existing (EdU-) oligodendroglia (OPCs: p=0.01, Mature: p=0.02, Intermediate p=0.44) and the population of newly-generated (EdU+) oligodendroglia (OPCs: p=0.02, Mature p=0.51, Intermediate p=0.07). **(F)** Quantification of the proportions of newly-generated (EdU+) vs pre-existing (EdU-) oligodendroglia overall (p=0.91) and at each lineage stage in the somatosensory cortex (OPCs p=0.15, Mature p=0.60, Intermediate p=0.36). B-F: n=4-5 mice/group, unpaired two-tailed t-test, data = mean $\pm$ SEM.